Proceedings World Geothermal Congress 2015
Melbourne, Australia, 19-25 April 2015

Synthesis of Well Test Data and Modelling of Olkaria South East Production Field

Daniel Saitet

Mailing address, P.O Box 785-20117 Naivasha, Kenya.

E-mail address, dsaitet@kengen.co.ke

Keywords: Olkaria, southeast, reservoir

ABSTRACT

Well data is analysed and reservoir parameters are interpreted unifying and incorporating the entirety of known knowledge and information into a single simplified conceptual model. The wells are highly permeable with convective zones appearing below 1 km depth in the zone immediately adjacent to Ololbutot lava flow. No independent magmatic heat sources are interpreted for the system but rather NW-SE and NNE-SSE trending faults act as fluid conduits allowing the fluid to percolated into the deep reservoir rock where it collects heat and localized upflow zones appear in the vicinity of OW-802 along permeable structures. The HOLA well bore simulator is used to predict well output curves for deep wells in the field. Most of the wells are fed by single phase liquid reservoir and therefore low outputs are expected. A resource assessment is carried out by Monte Carlo simulation which show average power output likely to be produced in the area is about 42 MWe and maximum possible output is shown to be in the region of 73 MWe using conventional flash power plant cycles. A natural state model for the field is constructed using TOUGH2. The model places plausible resource prospect areas along known structures in the area.

1. INTRODUCTION

Olkaria, a large volcanic complex, located at the axis of the Great East African Rift Valley, has formed the focus of geothermal exploration in Kenya for many years. Reconnaissance studies were commissioned to explore the area for geothermal resources in the early fifties. Numerous surface manifestations are prevalent in the area including fumaroles, altered grounds and sulphur deposits are believed to have attracted initial explorers to the area. It was not until 1956, when drilling started in the area. Two wells, OW-X1 and OW-X2 were drilled to 950 m depth with no success. The two wells were located close to an area which was most probably easily accessible and with great surface activity. Their failure to sustain discharge discouraged further drilling activity until the oil crisis when exploration for alternative energy sources gathered momentum. By this time, the government and the United Nations Development Program entered into a cooperation which supported additional exploration studies. Extensive Geo-scientific studies were carried out and proved the existence of exploitable resources at Olkaria.

The next well was located in the south east of Olkaria Hill and was drilled to a kilometre depth. OW-1 was not able to discharge despite being located in a geologically plausible location at the intersection of two major faults. A decision was then made to concentrate drilling efforts eastwards near the most recent lava flow. OW-2 was drilled next with great success. The well encountered temperature above 280°C and discharged high enthalpy fluids. Deep exploration wells were drilled thereafter near this well and culminated into commissioning of a 45MWe plant at Olkaria 1 which was fully operational by 1985.

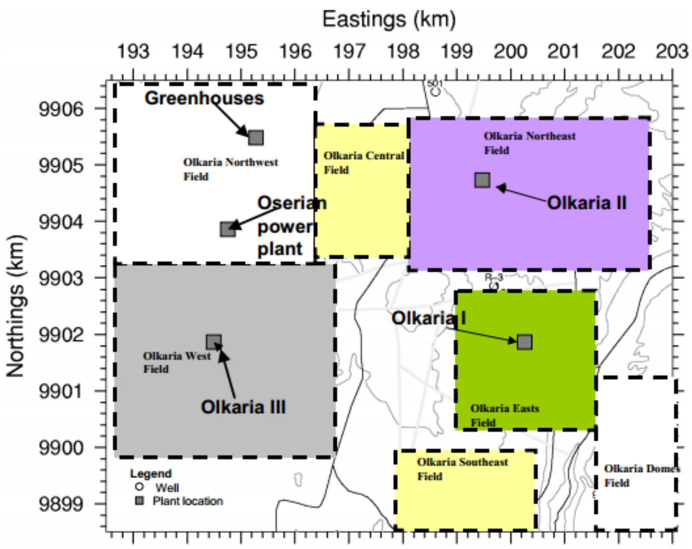

Figure 1: Olkaria geothermal field showing seven production sectors.

For further development in the area, a decision was reached to sub-divide the large field into seven sectors namely; Olkaria West (OWPF), Olkaria North West (ONWPF), Olkaria Central (OCPF), Olkaria North East (ONEPF), Olkaria East (OEPF), Olkaria South East (OSEPF) production fields and Olkaria Domes. The locations of the field sectors were decided relative to Olkaria Hill.

Further drilling activities were concentrated at the Olkaria West and North East fields where power plants with 110 MWe and 105 MWe respectively were subsequently built. Drilling at Olkaria Domes did not start until 1998 when the first well was drilled there. To date, many wells have been drilled in the Domes field and a power plant is presently under construction.

Olkaria South East is the subject of this work. Prior to drilling deep wells, the area was thought to be an outflow zone (Ouma, 2009) from the nearby Olkaria East field and therefore somewhat ignored in exploration for high temperature geothermal resources. A decision to re-inject hot brine from the Olkaria East production field to this area has also been envisaged more recently. To this end, two shallow re-injection wells were drilled near the unproductive well OW-801. These wells were meant to be used in case sites for re-injection near the field were either unavailable or as part of dynamic reinjection plan envisaged to become necessary upon completion of additional 140 MW power plant also under construction.

Recent deep drilling which commenced with the drilling of OW-802 has however revealed that this field could be productive. Well OW-11A drilled from the Olkaria East production field was directed under the Ololbutot lava flow turned out to be very impressive. More wells have now been cited and drilled in the area all giving positive results. It is however unfortunate that to date none of these wells has been flow tested yet. It is expected that further appraisal drilling will continue in this area at least in the near future before current wells can be flow tested. A critical review of available data is therefore necessary if drilling were to continue.

This paper therefore is focussed at synthesising available well test data to attempt at understanding the properties, geometry and nature of the reservoir there. This work, apart from attempting to model reservoir conditions at depth, is also aimed at estimating productivity of the wells already drilled and therefore estimates resource capacity.

1.1 Geology and Structural Setting

Olkaria is located at the floor of the central Kenyan rift about 150 km to the North East of Nairobi. The area is both geologically and structurally complex. The volcanic system is associated with an old central volcano which collapsed leaving a large caldera rim of approximately 5 km which is defined in part, by a ring fracture and by pumice domes. Rocks occurring on the surface are predominantly quaternary comendites, pumice fall and ash deposits of late Pliocene to Holocene. Some trachytic flows appear to the south of the geothermal area below thick pyroclastic covers associated with the Longonot and Suswa eruptives. Minor volcanic glass material also appears in a few localities.

Volcanic centres are structurally controlled. The main eruptive centre is the Olkaria hill with major structural features also contributing significantly. The Ololbutot and Gorge farm faults are such eruptive fissures. The most recent volcanic episode is associated with the Ololbutot fault which produced rhyolite flows dated about 250 years BP based on charred wood found under it (Clarke, et al 1990).

The lithostratigraphic structure in the area is nearly horizontal (Muchemi, 1999 and Brown, 1984). Based on rock cutting and cores, the general lithostratigraphy of the greater Olkaria complex can be divided into two with the axis separating the western sector from the eastern sector passing through Olkaria hill. Omenda (1998) discusses these formations and proposed nomenclature: Mau tuffs, Plateau trachytes, Olkaria basalts and Upper Olkaria volcanics. Mau tuffs were found to be unique to the western sector while the trachytes and basalts are unique to the eastern sector.Geothermal manifestations are structurally controlled. Hot grounds and fumaroles are located along fractures with intense activity found at their intersections. Production wells cited at these intersections prove to be particularly good.

Olkaria is a complex grid faulted area located at the vicinity of Western rift boundary faults of the rift system. Tectonic activity is associated with extensional rifting and consequent tension created North-South faulting along the axis of the rift. The dominant structures at Olkaria are the Ololbutot fault (North-South), the Gorge farm fault (North East-South West), the Olkaria Fault (East North East-West South West) and the Suswa fault (North East-South West). An alignment of eruptive domes is prominent to the east of the field probably demarcating a caldera rim and which has been mapped elsewhere around the greater volcanic complex. Many other buried faults with similar trends have been inferred by analysis of drill cores and rock cuttings. (Muchemi, 1998 and Omenda, 1998). Micro-seismic monitoring of Olkaria geothermal field has shown lineaments of epicentres similar to mapped structures (Simiyu and Keller, 1999). Intersections of these lineaments are associated with shallower and less prominent seismic events suspected to be consequent of fluid flow in the subsurface.

Olkaria South East field (OSEPF) is traversed by Ololbutot fault to the west, North West-South East trending fault passing through Ololbutot recent lava flow and is bounded to the east by the Olchorro Oirowua Gorge. Another prominent structure trends North North East-South South West intersecting with North West-South East fault at the close vicinity of well OW-804 in the OSEPF. A shorter parallel fault is also intersected by wells OW-804A and OW-802A drilled directionally to the South East. The inferred alignment of eruptive centres offers a natural boundary for the field to the south. The field is juxtaposed to the OEPF field which has produced for more than 30 years and the Domes field which is currently in the development phase. Figure 2 shows the structural map of the greater Olkaria geothermal field.

1.2 Well Conditions

1.2.1 Feedzones

Table 1 summarizes the temperature situation in all wells in this field and feedzone locations. Wells OW-802, OW-804 and OW-804A encounter temperatures above 280 °C while OW-802A and OW-803 reached temperatures in the range 230-240 °C as latest measured bottom-hole temperatures (BHT). All these temperatures are considered high and are not significantly lower than those encountered elsewhere in Olkaria. However, in the adjacent OEPF geothermal field, most wells produce from steam fed reservoirs at shallow depths and liquid zones at greater depths. This seem not be the case in these wells except for OW-802 which bears this resemblance. Deliverability of these wells can be limited by this fact. In some cases, at the Olkaria Domes field, marginal wells with similar profiles as these have turned out to be poor wells. However, wells in this field have appreciable higher permeability than their counterparts in the margins of the Domes field. Good examples of these wells are OW-917, OW-918 and OW-918. Pressure situations in OSEPF wells closely resemble observations elsewhere in Olkaria.

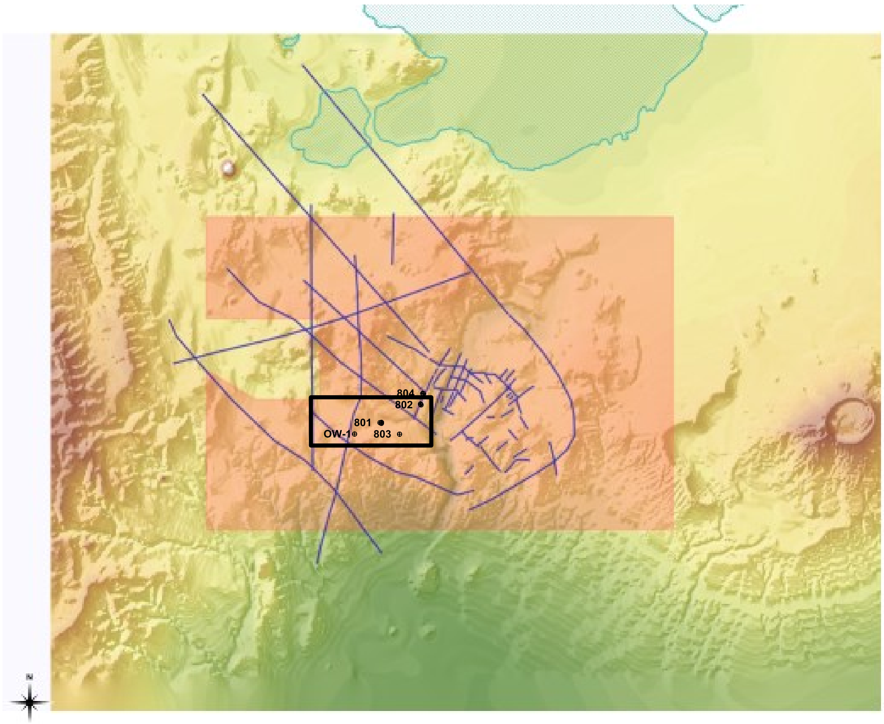

Figure 2: Structural map of Olkaria geothermal field. Inset is the Olkaria South East production field. The black dots show locations of drilled wells.

Table 1: Summary well temperature and feed zones.

Well name	Type	Depth TVD (m)	Casing shoe TVD (m)	Measured BHT (°C)	Main feedzone TVD (m)	Other feedzone TVD (m)
OW-1	Vertical	1003	418	126	...	...
OW-801	Vertical	2000	847	215	950	1350
OW-801 R1	Vertical	600	190	87	350	300 500
OW-801 R2	Vertical	640	266.7	103	500	350 550
OW-802	Vertical	3000	732.7	280	1050	850 1800 2000 2500
OW-802A	Directional N137E	2860	785.3	220	1800	850 2500
OW-803	Vertical	3000	861.68	230	1500	1300 1800 2500 2850
OW-804	Vertical	3000	782.65	300	1900	850 1500 2200 2900
OW-804A	Directional N145E	2870	796.7	280	2250	1200 1300 1450 2450

1.2.2 Physical Conditions

The early wells drilled in the OSEPF field were shallow and only penetrated into the sharp thermal gradient of the reservoir cap rock. OW-801 achieves some convective character at depth but which occurs at non-commercial temperatures. More recent deep drilling has proved the existence of a resource at least in the north-eastern margins of the field closest to known structures. The wells presently under study are located near significant structures in the area and are therefore likely to be reasonable producers. Reservoir temperature ranges from 230°C to 360°C with the highest located near known structures. Reservoir fluids are likely to be liquid dominated with boiling processes commencing only at the wellbores of wells OW-802, 802A, 803, 804A. It is notable however, that most of these wells have seldom reached stable formation conditions and therefore physical conditions may change with more recovery. Figure 3 shows the formation temperatures calculated from available warm up profiles. Some corrections are performed to compensate for effects of convection in the wellbores and short warm up periods in few cases.

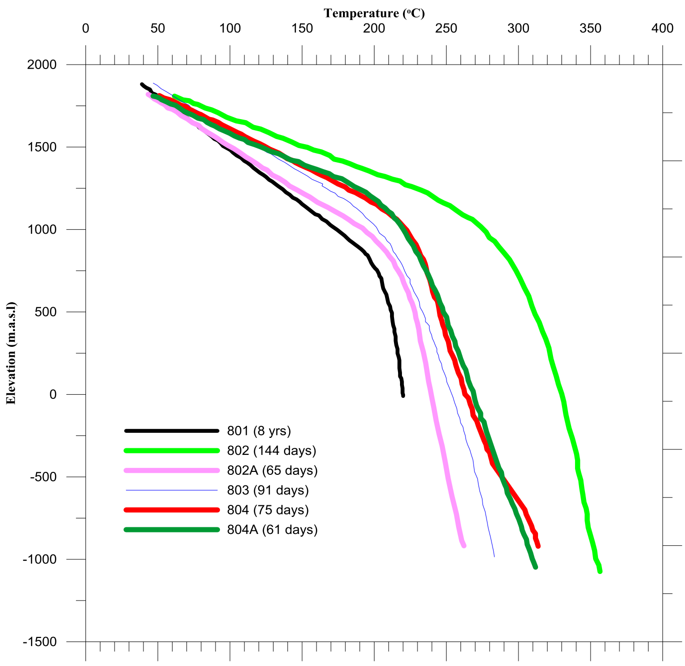

Figure 3: Formation temperature profiles.

1.3 Temperature Distribution

A Temperature profile is taken from well OW-1 and elongates in a NE directional ending at OW-804. The profile considers vertical wells falling in between. The temperature distribution along this profile is mushroom shaped centred around OW-802. The reservoir is capped around 1200 m.a.s.l. corresponding to about 700m depth where temperature rises sharply reaching over 300°C in just half a kilometre deeper. The hotter region gradually falls to greater depths towards the start of the profile. It can be generally confirmed here that temperature falls with distance away from OW-802. The existence of a deeper temperature barrier in the opposite direction is observable as well with slight temperature reduction observed in OW-804.

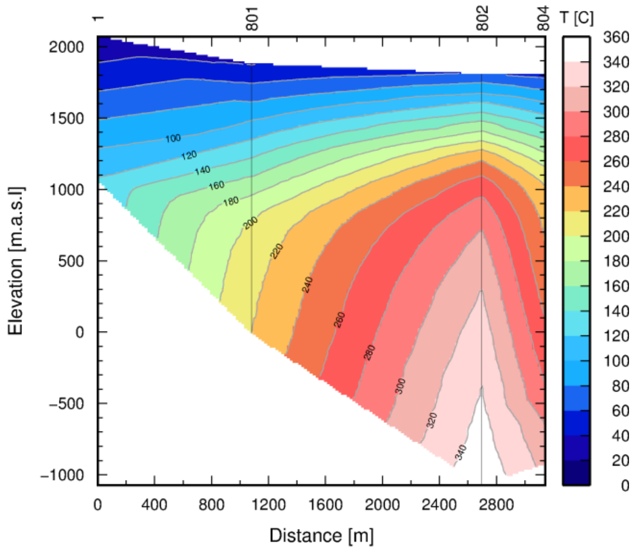

Figure 4: Temperature section along profile 1 (NE).

1.4 Pressure Distribution

Evaluation of initial pressure in this field shows all deep drill holes are in the somewhat similar pressure regime. Figure 5 shows these pressure profiles which lie approximately in the same range as in the Olkaria East field. OW-802 however departs slightly at great depths due to the influence of steam in the wellbore as it has heated up the longest. OW-802 is also located at the centre of the upflow region. Comparatively, these pressures agree reasonably well with initial reservoir pressure evaluated during injection testing. See next section 1.6.

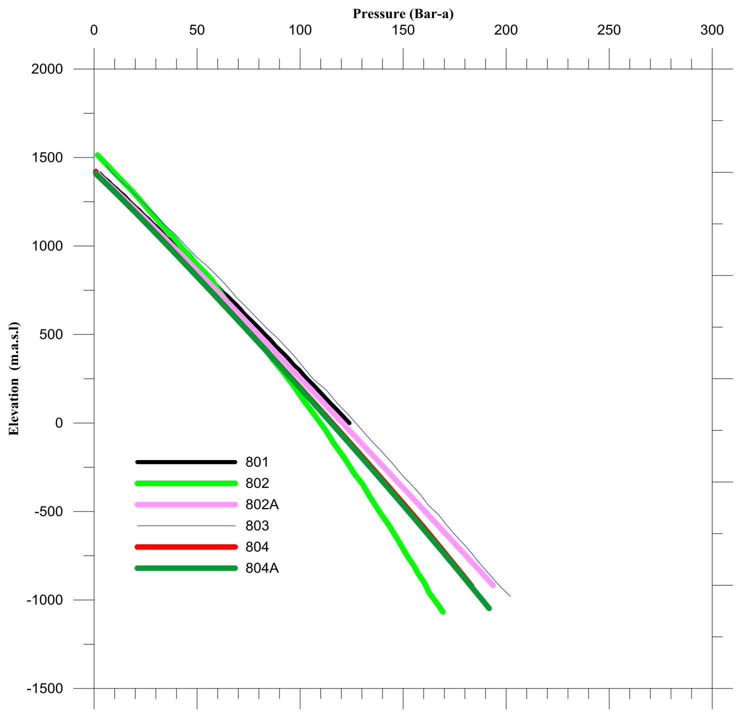

Figure 5: Initial pressure profiles.

1.5 Alteration Mineralogy

Composition of geothermal fluids are controlled by temperature depended on reactions between the rock and fluid. The resulting hydrothermal alteration products are affected by temperature, pressure, rock type (at low temperatures), permeability, fluid composition and duration (Brown, 1978). These minerals provide then a historical evolution of temperatures in the system.

Particular alteration minerals have been employed in different fields as a kind of geothermometer. While this is mainly field dependent, the Olkaria experience (Omenda, 1998) with mineral formation temperature does not differ largely with those observed elsewhere for example Reyes (2000) and are therefore adopted.

In this study two minerals were chosen for this purpose. The first appearance of epidote maps formation temperatures of 240°C being encountered and that of actinolite-biotite gives temperatures in excess of 280°C. First appearances of these minerals were plotted alongside established temperature profiles in the field. Figure 6 shows reasonable correlation between the two thermometers to the east of the field and a departure in the colder part of the field mainly in wells OW-801 and OW-803. In this sector of the study area, temperatures shown by mineralogy are much lower than actual measurements in drill holes. This is a consequence of cooling further away from the established upflow and known fluid conduits in the area.

1.6 Step-rate Injection Tests

Subsection Step-rate injection tests were carried out in all newly drilled wells. Pressure transient data is collected for different injection rates and analyses using Well Tester software. The results of these analyses are tabulated in Table 2. In general, the injection tests are considered successful despite there being few pressure recordings; a common limitation of mechanical tools. Pressure response of data is important in diagnostic exercises to deduce the nature of reservoirs, their sizes and boundary conditions existing. For simplicity, deep reservoirs were considered to be at an average of 240 ^{O}C and of the pressure range of 160 to 180 bar-a. The area actively exchanging reservoir fluids can be difficult to determine. An estimate of an average 500 m was considered reasonable for the purpose of this study. However, shallower wells had different consideration of reservoir thickness and expected temperature.

In analysis of injection tests, two kinds of models were considered for the reservoir, on one hand a homogeneous reservoir and on the other hand a dual porosity reservoir. Three different boundary conditions were used in the modeling, an infinite reservoir, a reservoir with constant pressure at the boundary and finally a no-flow boundary in which case the fluid cannot flow freely across the boundary, but in that case the pressure continues to increase with time when the injection rate is kept steady. Best results from the tests show the reservoir conforms to the homogeneous reservoir with constant pressure boundary and constant skin with wellbore storage.

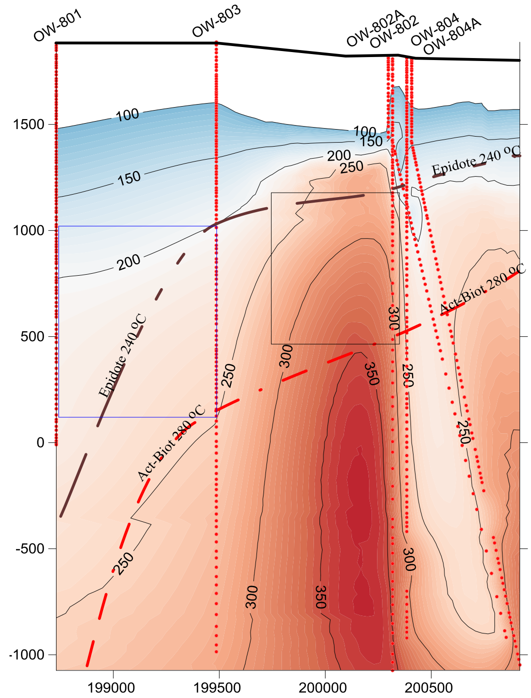

Figure 6: Relation between formation temperature and alteration mineralogy at OSEPF. Black dotted line shows first appearance of Epidote and red dotted line shows first appearance depths of Actinolite or Biotite. Blue rectangle shows regions of cooling and black shows regions of either equilibrium or heating.

Table 2: Well test analysis.

Well Name	Depth TVD (m)	Main Feedzone TVD (m)	II (all steps) (l/s.bar)	Best Step	Transmisivity $\times10^{-8}$ $m^3/(Pa\cdot s)$	Storativity $\times10^{-8}$ $m^3/(Pa\bullet m^2)$	Skin Factor	Well Bore Storage $\times10^{-4}$ m^3/Pa	II (Best Step) (l/s.bar)
OW-801 R1	600	350	4.75	4	3.06	1.14	-6.14	1.12	12.23
OW-801 R2	640	500	4.27	4	2.66	1.41	0.76	1.4	3.47
OW-802	3000	1050	6.95	1	0.74	6.65	-5	0.72	5.34
OW-802A	2860	1800	3.34	3	1.75	6.65	-1.87	0.47	2.92
OW-803	3000	1500	1.12	5	0.84	6.95	-3.15	0.59	1.75
OW-804	3000	1900	4.87	4	3.23	6.75	-2.08	5.55	7.51
OW-804A	2870	2250	4.28	4	6.3	6.75	0.41	5.56	7.23

1.7 Well Simulations

1.7.1 Theory

The flow of geothermal fluid flowing vertically in a well can be expressed using two sets of mathematical equations. Between the feed zones, the flow is represented by one dimensional steady state equations of momentum, energy and mass flux equations. In the case of a feed zone being encountered, mass and energy balances are then required between the fluid already in the wellbore and the incoming fluid. By applying boundary and initial conditions that fully describe the problem, the governing equations can then be solved numerically. The solutions to this equations involves taking small finite sections of the pipe from the origin of the fluid to the top thus a continuum from feed zone to wellhead is solved. It is also possible to solve the equations from top to bottom as well with an appropriate description of the flow.

The governing steady-state equations for mass, momentum and energy flux for a vertical flowing well is set up in Equations 1, 2, and 3)

$$\frac{d\dot{m}}{dz} = 0 \tag{1}$$

$$\frac{dP}{dz} - \{\left[\frac{dP}{dz}\right] fric + \left[\frac{dP}{dz}\right] acc + \left[\frac{dP}{dz}\right] pot\} = 0 \quad (2)$$

$$\frac{dE}{dz} \pm Q = 0 \quad (3)$$

where $\dot{m}$ = total mass flow
z = depth
P = pressure
E = total energy flux
Q = ambient heat loss over unit distance

In case, a feed zone is encountered, flow between the well and the reservoir gives the governing equation of the form, Equation 4

$$\dot{m}_{feedzone} = PI \left[\frac{k_{rl}\,\rho_1}{\mu_l} + \frac{k_{rs}\,\rho_{rs}}{\mu_s}\right] (P_r - P_l) \quad (4)$$

where $\dot{m}$ = flow rate from feedzone
PI = productivity index of feedzone
k_{rl} = relative permeability in liquid phase
k_{rs} = relative permeability in steam
ρ_l = density of liquid
ρ_{rs} = density
μ_l = dynamic viscosity of liquid
μ_s = dynamic viscosity of steam
P_r = reservoir pressure
P_l = well pressure

The HOLA well simulator presented by Bjornsson (1987) solves these equations for vertical wells from the bottom feed zone up the well. The bottom most feed zone need be at the bottom of the well and the flow into the well is defined as positive and the flow from the well outwardly into the formation takes the negative sign. Different computation modes are available in HOLA for simulations with different known parameters.

In this work, computation mode 2 was applied for predicting the output curves given known relative feed zone flow rates and calculated enthalpy conditions. The Orkiszewski velocity model (Orkiszewski, 1967) was assumed to describe the phase velocity in the wells.

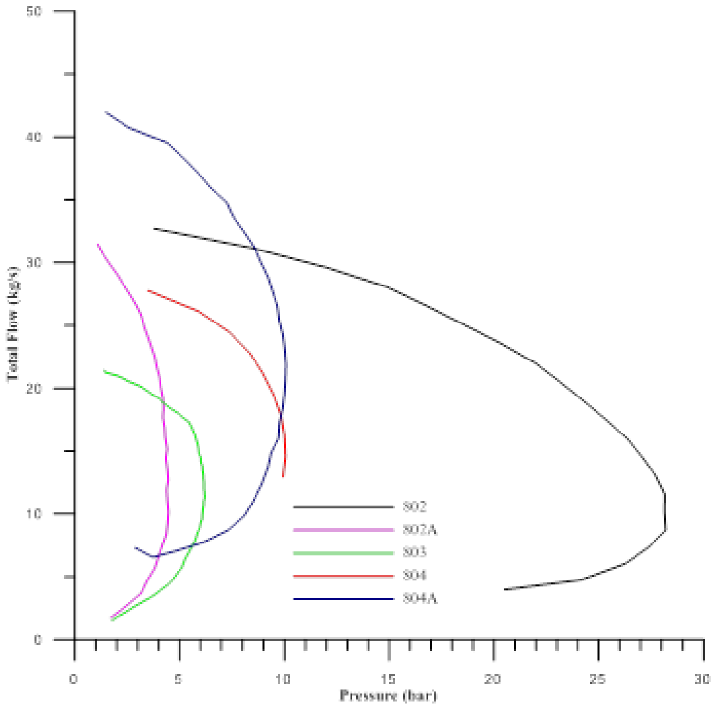

Figure 7: Calculated output curves.

1.7.2 Results

The program HOLA was used to estimate the productivity curve for candidate wells in OSEPF. The thermodynamic parameters used were calculated from observed pressure and temperature conditions during warm up discussed in section 3.1. The well productivity indices were estimated by taking the assumption that it equals a third of the well's injectivity indices (Grant and Bixley, 2011) and relative contributions assigned to the feed zones in the well.

Results show liquid wells producing at low pressure regimes with moderate deliverability (Figure 7).

2. CONCEPTUAL MODEL

Grant and Bixley, 2011 define conceptual models as descriptive models of geothermal systems incorporating, and unifying the essential parts of physical features of the system. Conceptual basis are constructed by unified interpretation of data available for a particular field. Incorporation of ideas and viewpoints from various disciplines and expertise are of essence in this task. Variable datasets are used in the construction of these models and depends on the phase of development; therefore amount of data available. Fields under exploration rarely have any datasets beyond surface geo-scientific data. In the case of fields that have some or many drill-holes conceptual models involve interpretation of a lot more data and are therefore considerably more detailed.

The Olkaria geothermal field has been studied extensively over the decades. New information is increasingly acquired with drilling of additional and deeper wells all of which have increased dramatically the knowledge of the system. Down-hole data is of paramount importance in providing calibrations to models developed earlier with little or no information about the different sectors of the field, its geometry, nature and boundaries. The Olkaria conceptual model proposed by West-JEC (2009) and improved by Mannvit/ÍSOR/Vatnaskil/Verkís Consortium (2011) describes the heat source of the system as of magmatic origin lying at shallow (6 km) depths with dyke intrusions which in turn are responsible for at least four up flow areas; one below the Domes, another below the OEPF, another below ONEPF and another below OWPF. Meteoric water from the high rift scarps percolate deep via deep seated faults dipping into the centre of the rift are heated on their way and up well along permeable structures.

A simple localized model of the OSEPF is developed and is presented in Figure 8. The analyses of temperature and pressure data in section 3 and 4 of this work are used to construct a conceptual model of the OSEPF. Geothermal fluids are permeated through the Ololbutot fracture zone and NW-SE faults intersecting it allowing water to percolate deep into the hot crust. The waters are heated, become lighter and flow towards the surface through permeable zones and structures. The greatest and hottest up flow is located near OW-802. The up-welled waters reach the impermeable cap rock above it where it is dispersed on either side of the mushroom-shaped up flow.

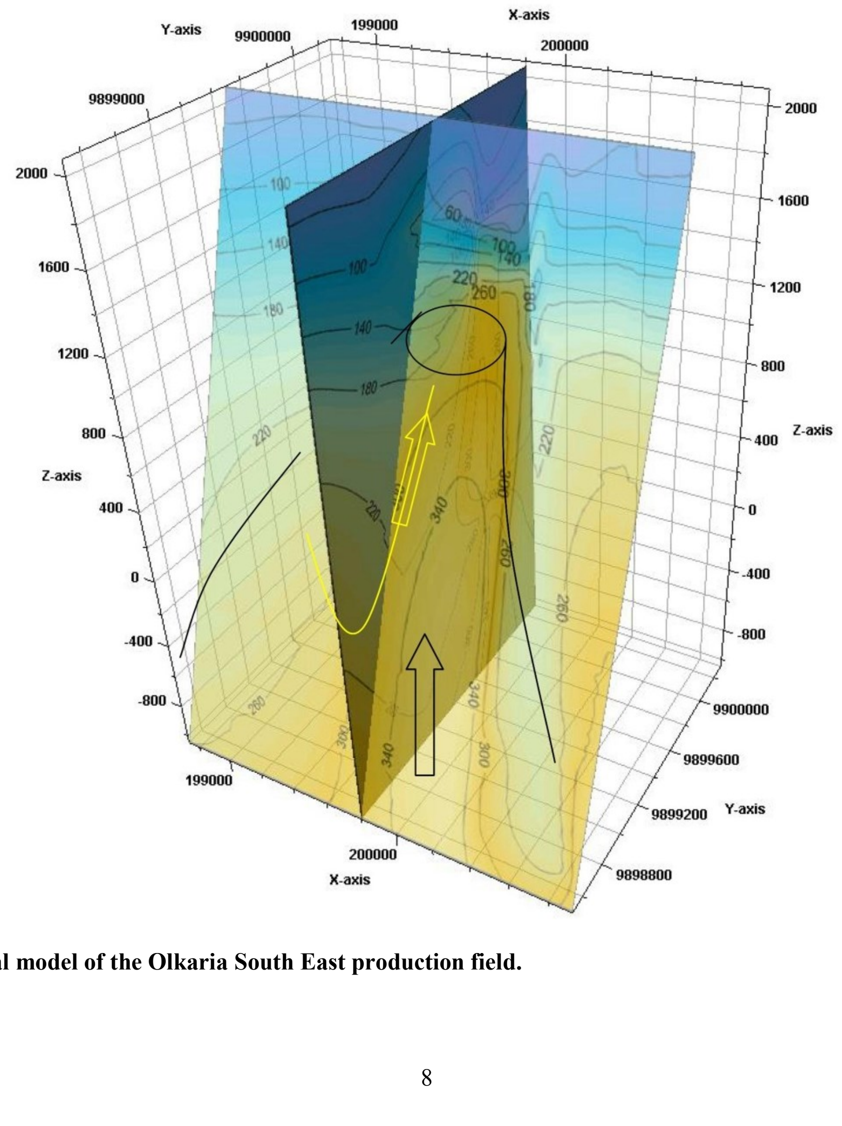

Figure 8: Conceptual model of the Olkaria South East production field.

3. NUMERICAL MODEL

3.1 The Computational Grid

A TOUGH2 model consists of a number of elements connected to each other in a grid. The described connections between the different elements in space are referred to as a grid. A simple grid was constructed for the OSEPF containing 1984 elements divided into 8 layers. The stratigraphic layers taken are construed to signify reasonable distribution of permeability and heat flow. Five different rock types are assigned to the layers. Figure 9 shows the general set up of the grid.

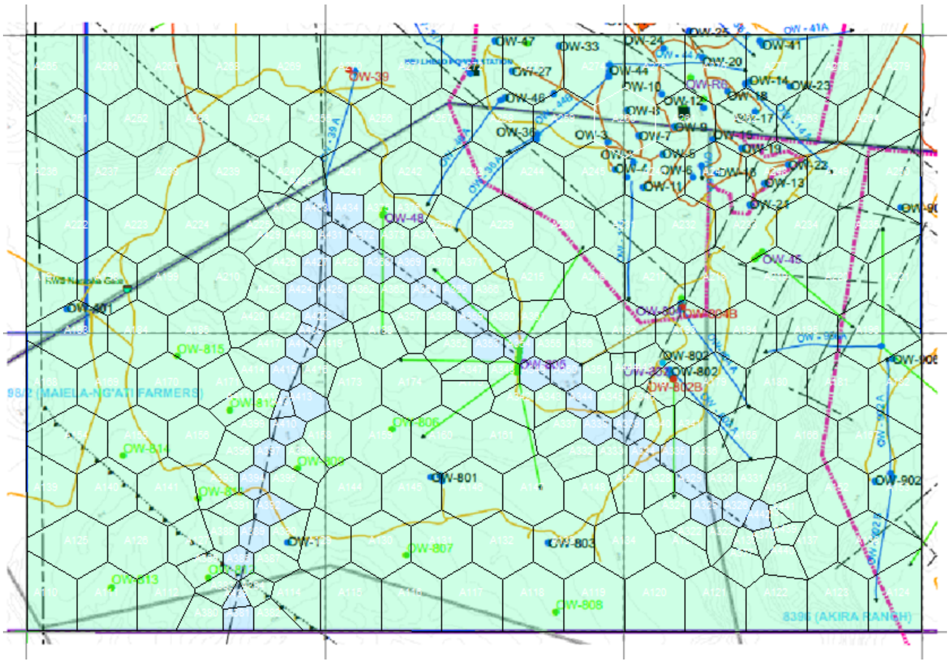

Figure 9: The computational grid.

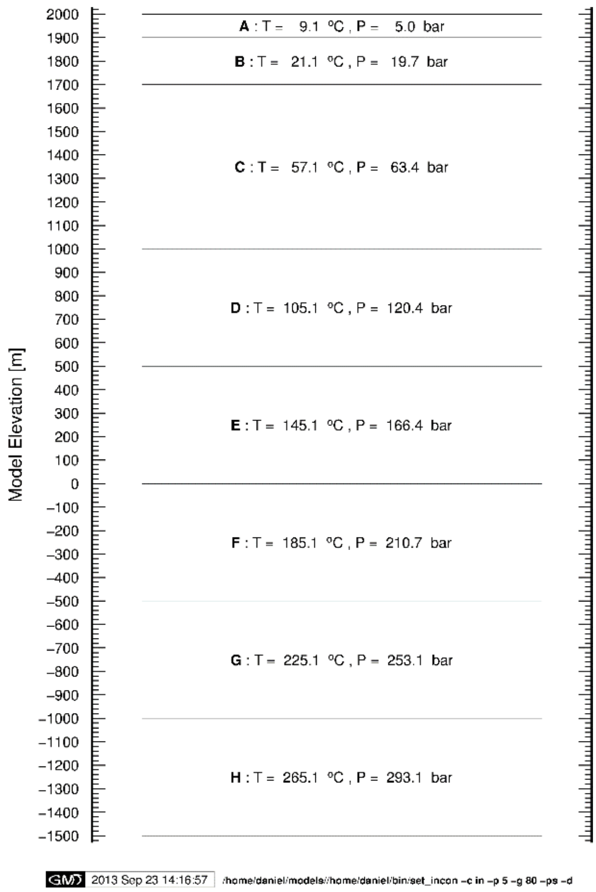

Figure 10: Vertical section of the grid showing initial conditions for each layer.

3.2 Initial Conditions

Initial conditions were calculated for the permeability and heat conductivity allowed for each domain. Simulations were then run to obtain steady state conditions for each element. Observed initial temperature and pressure conditions observed in well measurements are matched quite closely in this model. Layer A (topmost layer) was initially assigned temperatures of 19.1 ^{O}C and pressure 5 bar and based on a uniform thermal gradient of 80 °C/km temperature and pressure were assigned to all other layers as shown in Figure 10.

3.3 Natural State Model

Fluid sources are located in elements in the vicinities of established intersecting structures known to control fluid movements. Mass sources are assigned strengths of between 5-10 kg/s and steady state conditions are calculated where changes in the primary variables are small on the time-scale of several thousand years. Fumarole activity located in the vicinity of Ololbutot fault to the south-eastern margin of the field is simulated with a mass sink located in the vicinity of well OW-1 discharging at -0.0001 kg/s at 2500 kJ/kg. Temperature distribution at depths was matched to the key qualities evaluated in the preceding analysis of pressure and temperature by experimenting with different values for permeability and heat inflow to the system. To recall, the reservoir capping is set at about 1000 m.a.s.l. where onset of convection was observed. The convective temperatures varied of cause relative to the well location with respect to the centre of the upflow. Well OW-802 for example convects at about 320 ^{O}C while the well OW-804 convects at 280 ^{O}C. On the other hand, well OW-801 located outside this upflow only reaches around 200 ^{O}C. The Figure 11 shows the model temperature response at sealevel.

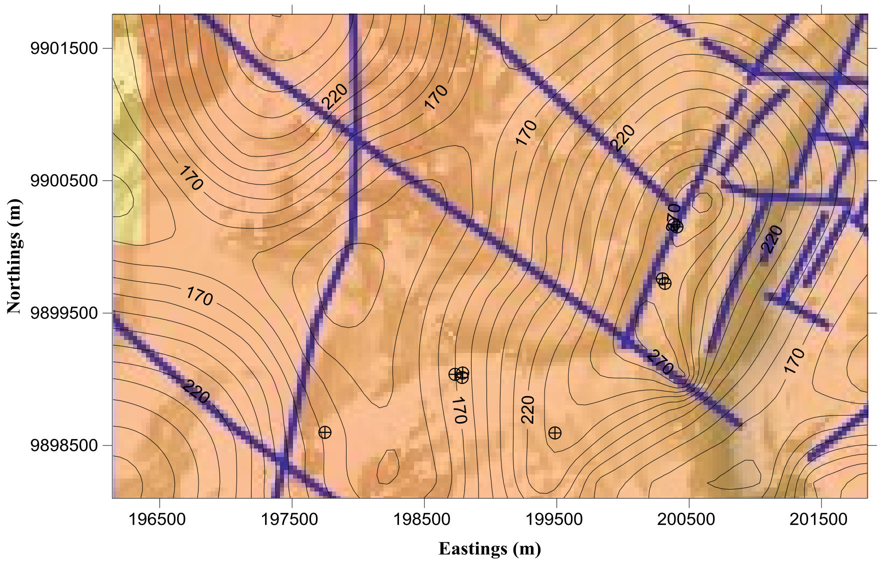

Figure 11: Model temperature contours at Layer F.

4. CONCLUSIONS

The OSEPF consists an upflow zone located beneath OW-802 and which domes to shallow depths at high temperatures and aligned in the NE-SW fashion. The system is narrow and is highly structurally controlled. The region west of well OW-803 is shown to be cooling and OW-801 and OW-1 are outside the high temperature geothermal system.

The reservoir is a homogeneous one with constant pressure boundaries interpreted to be sustained by recharge from the main structures in the field. Contrary to earlier hypotheses, the geothermal system is not sustained by outflow from the OEPF. On the contrary, it consists an independent hydrological system controlled mainly from fluid movement from the south northwards with NW-SE trending structured dominate fluid movement at depths.

No localized and independent magmatic heat sources are interpreted for this system but rather associated with similar magma heat under OEPF. Fluids travelling in the fractures present in the field encounter great heat at depth in the vicinity of the field and upwell at the intersections of grid faults located in the area. The hotter fluids are associated with the NW-SE trending structures passing through Ololbutot lava flow and cool away from it as permeability decreases. Cooler fluid is present in NE-SW fault intersected by OW-802A and OW-804A but contribute to significant convective zones in the said wells.

Plausible drilling targets are along the NW-SE trending faults. This work shows another possible drilling target is the south western margin of the field to the immediate west of Ololbutot fault. This locality is thought to contain hot fluids associated with the Suswa fault zone and the ring fracture.

REFERENCES

Björnsson, G.: A multi-feedzone geothermal wellbore simulator, Lawrence Berkeley Laboratory, report LBL-23546, (1987), 8-19.

Brown, P.R.L.: Hydrothermal alteration in active geothermal fields, *Annual Review in earth and planetary sciences,* **6**, (1978), 229-250.

Clarke, M. C. G., Woodhall, D. G., Allen, D. and Darling, G.: Geological, volcanological and hydogeological controls of the occurrence of geothermal activity in the area surrounding Lake Naivasha, Kenya, Ministry of Energy, Kenya and British Geological Survey, (1990), pp.138.

Grant, M.A and Bixley, P.F.: Geothermal reservoir engineering-second edition, Academic press, Burlington, USA, (2011), pp.359.

Mannvit/ÍSOR/Vatnaskil/Verkís Consortium: Revision of the conceptual model of the Greater Olkaria Geothermal System – Phase I. Mannvit/ÍSOR/Vatnaskil/Verkís, (2012), pp.100.

Muchemi, G.G.: Geothermal Exploration in the Kenyan rift, 20th Anniversary Workshop, Geothermal training programme, Reykjavik, Iceland (1998).

Omenda, P.A.: The geology and structural controls of the Olkaria geothermal system, Kenya, *Geothermics*, **27(1)**, (1998), 55-74.

Orkiszewski, J.: Predicting Two-Phase Pressure Drop in Vertical Pipe, *Journal Petroleum Technology*, **19**, (1967), 829-838.

Ouma, P.A.: Geothermal exploration and development of the Olkaria geothermal field, *Proceedings*, Short course IV on Exploration for Geothermal Resources, UNU-GTP, GDC and KenGen, at Lake Naivasha, Kenya, November 1-22, (2009).

Reyes, A.G.: Petrology and mineral alteration in hydrothermal systems: from diagenesis to volcanic catastrophes, UNU-GTP, Iceland, report 18-1998, (2000), pp.77.

West JEC: Olkaria optimization study (phase II), Final report (2009).